Hippocampal profiling: Localized magnetic resonance imaging volumetry and T2 relaxometry for hippocampal sclerosis

Vos, Sjoerd B ; Winston, Gavin P ; Goodkin, Olivia ; Pemberton, Hugh G ; Barkhof, Frederik ; Prados, Ferran ; Galovic, Marian ; Koepp, Matthias ; Ourselin, Sebastien ; Cardoso, M Jorge ; Duncan, John S

Abstract: OBJECTIVE Hippocampal sclerosis (HS) is the most common cause of drug-resistant temporal lobe epilepsy, and its accurate detection is important to guide epilepsy surgery. Radiological features of HS include hippocampal volume loss and increased T2 signal, which can both be quantified to help improve detection. In this work, we extend these quantitative methods to generate cross-sectional area and T2 profiles along the hippocampal long axis to improve the localization of hippocampal abnormalities. METHODS T1-weighted and T2 relaxometry data from 69 HS patients (32 left, 32 right, 5 bilateral) and 111 healthy controls were acquired on a 3-T magnetic resonance imaging (MRI) scanner. Automated hippocampal segmentation and T2 relaxometry were performed and used to calculate whole-hippocampal volumes and to estimate quantitative T2 (qT2) values. By generating a group template from the controls, and aligning this so that the hippocampal long axes were along the anterior-posterior axis, we were able to calculate hippocampal cross-sectional area and qT2 by a slicewise method to localize any volume loss or T2 hyperintensity. Individual patient profiles were compared with normative data generated from the healthy controls. RESULTS Profiling of hippocampal volumetric and qT2 data could be performed automatically and reproducibly. HS patients commonly showed widespread decreases in volume and increases in T2 along the length of the affected hippocampus, and focal changes may also be identified. Patterns of atrophy and T2 increase in the left hippocampus were similar between left, right, and bilateral HS. These profiles have potential to distinguish between sclerosis affecting volume and qT2 in the whole or parts of the hippocampus, and may aid the radiological diagnosis in uncertain cases or cases with subtle or focal abnormalities where standard whole-hippocampal measurements yield normal values. SIGNIFICANCE Hippocampal profiling of volumetry and qT2 values can help spatially localize hippocampal MRI abnormalities and work toward improved sensitivity of subtle focal lesions.

DOI: https://doi.org/10.1111/epi.16416

Hippocampal profiling: localised MRI volumetry and T2 relaxometry for hippocampal sclerosis

Sjoerd B. Vos[1,2,3,4,*,†], Gavin P. Winston[2,3,5,*], Olivia Goodkin[1,4], Hugh G. Pemberton[1,4,6], Frederik Barkhof[1,4,7,8,9], Ferran Prados[1,8,10], Marian Galovic[2,3,11], Matthias Koepp[2,3], Sebastien Ourselin[12], M. Jorge Cardoso[12], John S. Duncan[2,3]

[1]Centre for Medical Image Computing (CMIC), Department of Medical Physics and Bioengineering, University College London, London, United Kingdom
[2]Epilepsy Society MRI Unit, Chalfont St Peter, United Kingdom
[3]Department of Clinical and Experimental Epilepsy, University College London, London, United Kingdom
[4]Neuroradiological Academic Unit, UCL Queen Square Institute of Neurology, University College London, London, United Kingdom
[5]Department of Medicine, Division of Neurology, Queen's University, Kingston, Canada
[6]Dementia Research Centre, UCL Queen Square Institute of Neurology, University College London, London, United Kingdom
[7]Lysholm Department of Neuroradiology, National Hospital for Neurology and Neurosurgery, UCLH NHS Foundation Trust, London, United Kingdom
[8]Queen Square MS Centre, Department of Neuroinflammation, UCL Queen Square Institute of Neurology, Faculty of Brain Sciences, University College London, London, United Kingdom
[9]Department of Radiology & Nuclear Medicine, VU University Medical Center, Amsterdam, the Netherlands
[10]E-health Centre, Universitat Oberta de Catalunya, Barcelona, Spain
[11]Department of Neurology, University Hospital Zurich, Zurich, Switzerland
[12]School of Biomedical Engineering and Imaging Sciences, King's College London, London, United Kingdom
[*]These authors contributed equally

[†] Corresponding author
Sjoerd B. Vos
8.08 Malet Place Engineering Building
University College London
WC1E 6BT London
United Kingdom
s.vos@ucl.ac.uk

Keywords: hippocampal volumetry, relaxometry, neuroimaging, hippocampal sclerosis
Pages: 12; words: 2789; Figures: 6; Tables: 0

Abstract (289/300 words)

Objective: Hippocampal sclerosis (HS) is the most common cause of drug-resistant temporal lobe epilepsy, and its accurate detection is important to guide epilepsy surgery. Radiological features of HS include hippocampal volume loss and increased T2 signal, which can both be quantified to help improve detection. In this work, we extend these quantitative methods to generate cross-sectional area and T2 profiles along the hippocampal long axis to improve the localisation of hippocampal abnormalities.

Methods: T1-weighted and T2 relaxometry data of 69 HS patients (32 left, 32 right, 5 bilateral) and 111 healthy controls were acquired on a 3T MRI scanner. Automated hippocampal segmentation and T2 relaxometry were performed and used to calculate whole-hippocampal volumes and estimated quantitative T2 (qT2) values. By generating a group template from the controls, and aligning this so that the hippocampal long axes were along the anterior-posterior axis, we were able to calculate hippocampal cross-sectional area and qT2 in a slice-wise method to localise any volume loss or T2 hyperintensity. Individual patients were compared with normative data generated from the healthy controls. Twenty controls were rescanned for repeatability estimates.
Results: Profiling of hippocampal volumetric and qT2 data could be performed automatically and reproducibly. HS patients generally showed widespread decreases in volume and increases in T2 along the length of the affected hippocampus. Patterns of atrophy and T2 increase in the left hippocampus were similar between left HS and bilateral HS, and similarly for the right hippocampus between right HS and bilateral HS. These profiles have potential to distinguish between sclerosis affecting volume and qT2 in the whole or parts of the hippocampus.
Significance: Hippocampal profiling of volumetry and qT2 values can help spatially localise hippocampal MRI abnormalities and work towards improved sensitivity of subtle focal lesions.

Key points:

- Hippocampal sclerosis (HS) is radiologically characterised by atrophy and increased T2-weighted signal
- Quantification of these features improves sensitivity but utility may be limited if only providing one value for the whole hippocampus
- Localised quantification through profiling along the anterior-posterior hippocampal axis can be automated reliably and reproducibly
- This hippocampal profiling can be used as an additional tool towards improved characterisation, and possibly diagnosis, of HS

Introduction

Hippocampal sclerosis (HS) is the most common cause of medically refractory temporal lobe epilepsy (TLE) (Blumcke 2009), and surgical resection has a high chance of achieving seizure freedom (Wiebe 2001, De Tisi 2011). HS typically manifests radiologically as loss of volume, loss of internal architecture, and T2-hyperintensity (Van Paesschen 2004). MRI protocols used to visualise HS include high-resolution T1-weighted imaging to detect volume loss (atrophy) and T2-weighted or T2-FLAIR scans showing the latter two hallmarks (Jackson 1993a). Atrophy has been shown to correlate with seizure onset laterality (Bernasconi 2003) and seizure outcome after anterior temporal lobe resection (ATLR) (Schramm&Clusmann 2008). T2 abnormalities can be present even if there is no hippocampal volume reduction, and have been reported as the most consistent MRI finding in HS (Meiners 1994).

Quantitative evaluation of atrophy and T2 hyperintensities, using hippocampal volumetry and T2 relaxometry, can yield a higher sensitivity to detect HS than qualitative visual inspection (Jackson 1993a, Watson 1997, Coan 2014). Volumetry can help distinguish between normal and abnormal volumes in cases that may be difficult to classify visually (Jackson 1993b). T2

relaxometry, also called quantitative T2 (qT2)measurements, can be used to give an objective reflection of the T2 relaxation properties of the tissue.

In recent years, both volumetry (Winston 2013) and T2 relaxometry (Winston 2017) methods have been automated, enabling routine clinical use in comparing a patient's individual values to a normative database of healthy control subjects. These methods, however, only yield a single volume and qT2 value per hippocampus and may be insensitive to subtle focal abnormalities (Woermann 1998). In this work, we present an automated method to generate subject-specific localised volume and qT2 profiles along the hippocampal long axis to overcome this limitation. The software is made freely available as an extension of the online Web-based HippoSeg (Winston 2013, Prados 2016) service (http://niftyweb.cs.ucl.ac.uk/program.php?p=HIPPOSEG).

Methods

Data acquisition

Subjects underwent imaging on a 3T GE Discovery MR750 scanner with a 32-channel coil. Sequences included a three-dimensional (3D) T1-weighted inversion-recovery fast spoiled gradient recalled echo (TE/TR/TI 3.1/7.4/400 ms, field of view (FOV) 224×256×256 mm, matrix 224×256×256, parallel imaging acceleration factor 2) and a coronal dual-echo fast recovery fast spin echo proton-density/T2-weighted (TE 30/119 ms, TR 7600 ms, FOV 220×220 mm, matrix 512×512, slice thickness 4 mm, SENSE factor 2).
For patients, this was part of their routine clinical MRI protocol which also included a 3D T2-FLAIR (as in Vos et al., 2018) which was presented to radiologists for reporting.

Subjects

We expanded our healthy controls group with respect to Winston et al. (Winston 2017) to 111 healthy controls (age μ±σ 40.0±12.8, range 17.0-66.6 years; 52M/59F) without any history of neurologic or psychiatric disease, from previously scanned subjects. The study was considered a service improvement using clinically acquired data by the National Hospital for Neurology and Neurosurgery and the Institute of Neurology Joint Research Ethics Committee. Informed written consent was obtained from control subjects.

We included 69 patients (age μ±σ 42.7±14.7, range 18.0-76 years; 31M/38F) who had undergone brain MRI with an epilepsy protocol as part of routine clinical practice for TLE at the Epilepsy Society MRI Unit, Chalfont St Peter, and which been reported by a neuroradiologist as showing unilateral or bilateral HS on visual assessment and concordant with neurological examination. This consisted of 32 left HS (LHS), 32 right HS (RHS), and five bilateral HS (BHS).

Further, we reviewed all cases having undergone temporal lobe epilepsy surgery in our centre who had pathologically confirmed HS but without mention of HS in the radiological report. From those who had all sequences mentioned above, this yielded five subjects (see Supplementary Table S1 for details)

Image processing

Automated volumetry and T2 relaxometry was performed as described previous in Winston et al., 2013 and 2017, respectively. In brief, this used a multi-atlas-based algorithm for the

segmentation (STEPS; Cardoso 2013) using the 3D-T1 images, which was then coregistered to the PD/T2 scan and used as a mask to obtain qT2 values in. Hippocampal volumes were corrected for total intracranial volume (TIV) as in Winston et al. (Winston 2013).

The processing to obtain profiles along the anterior-posterior (AP) axis of the hippocampus then consists of 1) the generation of a group template; 2) registration of individual scans; 3) creating a normative database; 4) creating disease group average; and 5) comparing individual subject scans to that normative database.

1) Group template generation

The hippocampal regions of interest (ROIs) from the Harvard-Oxford atlas of the MNI-152 template were extracted, and using principal component analysis, their long axis was obtained. The MNI-152 template was then reoriented so that the hippocampal ROIs were along the AP axis (Figure 1a). The 3D-T1 scans of all 111 healthy controls were then registered to this rotated MNI template in an iterative manner using ten affine registration steps and ten nonlinear (fast free-form deformation) registration steps to obtain a population-specific group average template. All registrations were done in the open-source NiftyReg software package (Figure 1b) (Modat 2010, Modat 2014). For use in the later steps, a distance-map along the AP axis of this template was generated (Figure 1c), from the most posterior slice to the most anterior slice (distances 1-218 mm, respectively). The hippocampal segmentations from the healthy controls were transformed to the group template with the obtained transformation parameters. Voxels were included in the group-wise hippocampal masks when they were included in at least half the individual segmentations.

2) Registration of individual scan to template

Each subject's 3D-T1 scan was registered to the group template by a rigid registration to ensure similar orientations across subjects for visual comparison and symmetric alignment of the hippocampal long axes with the AP-axis. For accurate matching to the group template, each subject's 3D-T1 was non-rigidly registered to the group template by first a full affine registration to account for scaling between different head sizes, followed by a nonlinear registration to account for morphological differences between subjects. Importantly, this nonlinear registration was optimised by only evaluating the cost-function in the registration in the brain excluding the hippocampal segmentations from the template; this was done to avoid influence of atrophy or other pathology on the registration (Figure 1c). The registrations were then inverted to obtain the transformation from the template to the subject's T1 scan. The distance map from step 1 was then transformed to the subject's T1. For each coronal slice in the subject's hippocampal segmentation, the distances were averaged to obtain a mapping from the AP-location in the template to the subject's scan (Figure 1d). Cross-sectional areas (CSA) – corrected for TIV – were calculated for each slice, which together with the distances provides a single-subject profile.

For the T2 relaxometry, the transformation from the template to the T1 was concatenated with the rigid transformation from the T1 to the PD/T2 scan (Winston 2017). Similarly, the template distance map was transformed to obtain a mapping of location, and averaged within the hippocampal segmentation in the PD/T2-space.

3) Normative database generation

To generate a normative range with which to compare individual patient profiles to, all 111 healthy volunteers' CSA and T2 profiles were used. At steps of one millimetre along the AP-axis, the means (μ) and standard deviations (σ) of the hippocampal CSA and qT2 were calculated using a kernel density estimator. These were used to generate a normative range (μ ± 1.96*σ) of CSA and qT2 at each point along the AP axis of the hippocampus.

4) HS group averages

To compare TLE patient groups to controls in a group-wise fashion, step 3) was repeated for each of the LHS, RHS, and BHS groups.

5) Comparison of individual profiles

To compare individual subject profiles to the normative database from step 3), the same registrations as in step 2) were used. For the CSA, which originates from a 1 mm isotropic scan, the subject's profile is shown as a continuous profile to be compared to the normative data (μ ± 1.96*σ). For the qT2 values, calculated from a 2D acquisition with 4 mm slice thickness, the data points from each slice are shown.

Interscan reproducibility

To investigate scan-rescan reproducibility of the profiles, twenty controls that were scanned twice were processed and compared. The CSA and T2 profiles were subtracted from each other at each point, and the same kernel density estimation method as above was used to estimate the scan-rescan variability by estimating differences between in CSA and T2 values from the two scans at each point along the AP-axis.

Statistical interpretation

Whole hippocampal volumes and qT2s were compared using ANOVA between the four groups, and post-hoc t-tests between two groups if group-level differences were detected.
Statistical comparisons were performed at each point along the AP-axis comparing the normative range (from the 111 control subjects) to the three patient groups. For any point along the AP axis, the CSA was said to be smaller if the subject profile fell below the normal range (i.e., CSA < μ-1.96*σ). For the T2 measurements, this was if the subject profile showed higher qT2 than the normal range (i.e., qT2 > μ+1.96*σ). For group comparisons, the mean profile of the HS subtypes was compared to the normative range. For individual comparisons, the percentages of individuals with an abnormal profile was calculated for each point along the normative profile.

Results

An example profile of a healthy control is shown in Figure 2, which two example cross-sectional cuts through the hippocampal segmentation at the head and body. The closest corresponding slices from the T2 map are shown as well.

Average hippocampal volumes were reduced ipsilaterally and qT2 values were increased bilaterally in the unilateral HS patients, whereas there were bilateral volume and qT2 changes in bilateral HS patients (Supplemental Table S2). Comparing the CSA and qT2 profiles of the three patient groups to the normative data shows that on average sclerotic hippocampi had significantly decreased CSA along a large proportion of the length (Figure 3). On a group level,

the ipsilateral hippocampus in LHS was more atrophic than the ipsilateral hippocampus in RHS (Figure 3). Similarly, in BHS, the left hippocampus was more atrophic than the right. This asymmetry was less obvious in the qT2 values. There is a bigger portion of the sclerotic right hippocampus (in RHS and BHS) with increased qT2 compared to the left hippocampus (in LHS and BHS).

From the control group, 20 subjects were scanned again for test-retest analysis of both the imaging protocols and the analysis methods. A comparison of the standard deviation over the entire control population (n=111) and the intra-subject scan-rescan variation show the same spatial patterns, with CSA repeatability much higher than inter-subject variation (Figure 4).

Regarding whole-hippocampal volumes, the ipsilateral hippocampus was significantly atrophic in 29/32 (90.6%) of both LHS and RHS cases, with 4/5 (80%) and 5/5 (100%) of left and right hippocampi in BHS patients, respectively, atrophic. For whole-hippocampal qT2, ipsilateral hippocampi with significantly elevated qT2 were present in 18/32 (56.3%) LHS and 21/32 (65.6%) RHS patients, with 3/5 (60%) of left and 5/5 (100%) of right hippocampi affected in BHS. Figure 5 shows example CSA and T2 profiles for one LHS and one RHS patient in which no whole-hippocampus abnormalities were detected. These profiles demonstrate the benefit of analysing volumetry and qT2 values in more detail: for instance, confirming borderline normal/abnormal cases and providing more specific localisation.

In the patients where no radiological diagnosis of HS was made, but where resection did prove histopathological evidence of HS, three cases had dual pathology including HS, and two only HS (Table S1). For two of these patients, the CSA and qT2 profiles were indicative of hippocampal abnormalities, as shown in Figure 6. For patient 4, signal alterations were remarked upon in radiological review but not deemed clinically significant. These alterations were picked up with three slices of 4 mm thickness showing significantly increased qT2 corresponding with localised asymmetry in volume.

Discussion

In this study we presented an automated processing framework to look at localised hippocampal volumetry and T2 relaxometry by visualising this along the anterior-posterior axis. We observed group differences between LHS, RHS, and BHS with respect to a large group of healthy controls. These differences in cross-sectional area and qT2 are widespread and provide a more detailed representation of the quantitative imaging compared to single values for each hippocampus. These analyses and visualisations can be used in single-subject investigations.

<u>Group differences</u>

There is no evidence for different patterns of atrophy between the affected hippocampi in those with unilateral and bilateral HS, with very similar CSA profiles in the left hippocampus in LHS and BHS, and the right hippocampus in RHS/BHS (Figure 3). We found that in unilateral HS the significantly increased qT2 in the contralateral side (Table S2; Winston 2017) is a mild widespread increase, thus providing further support for either drug-related or seizure-related changes (Jackson 1993a, Scott 2003).

<u>Spatial variability</u>

Previous efforts towards qT2 profiling in the hippocampus had demonstrated a spatial gradient with qT2 higher anterior than posterior in both controls and patients with HS (Woermann 1998). Our results do not show such gradients. The methodology between Woermann et al., and this work is significantly different, with imaging and processing improved over time. In our current work: 1) image resolution is higher (voxel volume 0.74 mm^3 vs. 4.40 mm^3); 2) we sample the entire hippocampus rather than a small manually placed region; 3) we exclude any partial volume voxels (as in Winston 2017); and 4) had a bigger control population (111 vs. 20); all of which could potentially remove the apparent spatial gradient seen in Woermann et al., 1998.

The widespread abnormalities observed in this work (Figure 3) are concordant with evidence from both histopathology and imaging research indicating abnormalities in the CA1-CA3 subfields and dentate gyrus which run most of the length of the hippocampus (e.g., Briellman 2002, Von Oertzen 2002, Stefanits 2017) - for comparison of the orientations of these subfields to the CSA profiles please see Figure S1. Using automated tools for hippocampal subfields segmentation (Iglesias 2015, Yushkevich 2015), group-level differences in these subfields are also observed (Sone 2016), but patient-specific results at 3T or 7T have so far remained inconclusive as to the use in either improved detection of HS or prediction of post-operative seizure outcome (Voets 2017, Kreilkamp 2018, Shah 2019).

Increased variability of both CSA and qT2 in the control population around the hippocampal head is also seen in the test-retest analyses, and could be caused by residual imperfections in correcting for different lengths of hippocampi. The fact that the overall scan-rescan variability is 25-30% of the inter-subject variation is an indication of how reproducible these CSA profiles are. The intra-subject and inter-subject variation in the T2 profiles is almost identical, in both spatial variation along the long axis as well as magnitude. The higher scan-rescan variability here is likely to come from different slice positions, with 4 mm slices inherently causing greater scan-rescan variability than the isotropic 1mm acquisition of the 3D-T1. The increased variability in qT2 in the hippocampal head is expected to arise from the underlying anatomy, where the folded structures include small layers of CSF that increase voxel-wise qT2 which our partial volume correction (Winston 2017) might not solve fully.

Generalisation

This methodology has been made publicly available online, by extending the existing HippoSeg web-based service (http://niftyweb.cs.ucl.ac.uk/program.php?p=HIPPOSEG) to include CSA profiling (Winston 2013, Prados 2016). To account for inter-scanner differences in acquisition protocols, we have included two publicly available MRI datasets to the online tool to almost triple the normative database to enhance generalisability to other centers (See Online Supporting Information for more details). The T2 relaxometry sequence is likely to be more varied with scan set-up, and the lack of use outside of dedicated epilepsy imaging centers means there are no available datasets online. We have therefore not included this in our online tool.

Limitations

One of the limitations of the used methodology arises from the inherent issue of modelling the T2 relaxometry as a single qT2 value per voxel. This disregards any partial volume effects, and increases the variability in the measurements – especially in the head of the

hippocampus. The 4 mm thick slices increase increasing partial voluming, but was necessary to achieve sufficient signal-to-noise ratio for reliable qT2 quantification.
Validation of these tools is complicated by a lack of a full ground-truth of the whole hippocampus. Firstly, hippocampal resections for mesial TLE typically only resect the anterior 2 cm of the hippocampus (Galovic 2019), limiting the available histology. We therefor recommend the use of this methodology as an adjunct to expert radiological and neurological review.
The patient selection criteria for the large cohort used in this study was based on review of radiological reporting, selecting confirmed or suspected HS cases. This may also have resulted in demonstrating the profiling method more as a tool for improved characterisation rather than improved diagnosis of subtle HS, even if improved sensitivity over whole-hippocampal quantification was demonstrated (Figure 5).

Clinical utility

The potential clinical utility of this method is three-fold. Firstly, to identify subtle, especially focal anterior, HS that may be overlooked by visual reading. Secondly to offer the possibility of a restricted hippocampal resection, sparing structurally normal hippocampal tissue that may be contributing usefully to memory function (Sidhu 2016). Third, to identify subtle bilateral HS that may not be reported on visual reading, and which may militate against hippocampal resection.

Implications & Future work

The presented automated subject-specific analysis has been designed to integrate into a quantitative imaging setup of 3D-T1 and T2 relaxometry already recommended for routine clinical imaging in TLE patients (Coan 2014, Bernasconi 2019). The personalised approach taken in this work is specifically intended to facilitate integration into patient-based clinical research settings, hence the visualisation approaches taken to compare profiles to a normative database. In this, it is different from many recent approaches designed for group-based analyses (e.g., Goubrain 2015, Sone 2016, Yoo 2019, Hakimi 2019, Costa 2019). We suggest that this method may increase sensitivity, specificity, and/or localisation (as indicated in Figures 5 and 6) when used in radiological reporting or epilepsy surgery multi-disciplinary team discussions. Further evaluation in other patient populations is now warranted.

Conclusions

Localised volumetry and relaxometry measures of the hippocampus are possible to extract in a reliable and reproducible manner. CSA profiling is freely available online for widespread use.

References (max 50)

Blumcke I, Neuropathology of focal epilepsies: a critical review. Epilepsy Behav. 2009;15(1):34-39

Wiebe S, Blume WT, Girvin JP, Eliasziw M, for the Effectiveness and Efficiency of Surgery for Temporal Lobe Epilepsy Study Group. A randomized, controlled trial of surgery for temporal-lobe epilepsy. N Engl J Med 2001; 345: 311–18.

De Tisi J, Bell GS, Peacock JL, et al. The long-term outcome of adult epilepsy surgery, patterns of seizure remission, and relapse: a cohort study. Lancet 2011;378:1388-95.

Van Paesschen W. (2004) Qualitative and quantitative imaging of the hippocampus in mesial temporal lobe epilepsy with hippocampal sclerosis. Neuroimaging Clin N Am 14:373–400, vii.

Jackson GD, Connelly A, Duncan JS, et al. Detection of hippocampal pathology in intractable partial epilepsy: increased sensitivity with quantitative magnetic resonance T2 relaxometry. Neurology 1993;43: 1793–1799.

Bernasconi N, Bernasconi A, Caramanos Z, Antel SB, Andermann F, Arnold DL. (2003) Mesial temporal damage in temporal lobe epilepsy: a volumetric MRI study of the hippocampus, amygdala and parahippocampal region. Brain 126:462–469.

Schramm J, Clusmann H. (2008) The surgery of epilepsy. Neurosurgery 62 (Suppl. 2):463–481.

Meiners LC, van Fils A, Jansen GH, et al. Temporal lobe epilepsy: the various MR appearances of histologically proven mesial temporal sclerosis. Am J Neuroradiol 1994;15:1547-1555.

Watson C, Jack CR Jr, Cendes F. (1997) Volumetric magnetic resonance imaging. Clinical applications and contributions to the understanding of temporal lobe epilepsy. Arch Neurol 54:1521–1531.

Coan AC, Kubota B, Bergo FP, et al. 3T MRI quantification of hippocampal volume and signal in mesial temporal lobe epilepsy improves detection of hippocampal sclerosis. AJNR Am J Neuroradiol 2014;35:77–83.

Jackson GD, Berkovic SF, Duncan JS, et al. Optimizing the diagnosis of hippocampal sclerosis using MR imaging. AJNR Am J Neuroradiol 1993;14:753–762.

Winston GP, Cardoso MJ, Williams EJ, et al. Automated hippocampal segmentation in patients with epilepsy: available free online. Epilepsia 2013;54:2166–2173.

Winston GP, Vos SB, Burdett JL, Cardoso MJ, Ourselin S, Duncan JS. Automated T2 relaxometry of the hippocampus for temporal lobe epilepsy. Epilepsia 2017;58(9):1645-1652.

Woermann FG, Barker GJ, Birnie KD, et al. Regional changes in hippocampal T2 relaxation and volume: a quantitative magnetic resonance imaging study of hippocampal sclerosis. J Neurol Neurosurg Psychiatry 1998;65:656–664.

Prados F, Cardoso MJ, Burgos N, et al. NiftyWeb : web-based platform for image processing on the cloud. International Society for Magnetic Resonance in Medicine (ISMRM), 24th Scientific Meeting and Exhibition, Singapore, 2016.

Vos SB, Micallef C, Barkhof F, et al. Evaluation of prospective motion correction of high-resolution 3D-T2-FLAIR acquisitions in epilepsy patients. Journal of Neuroradiology 2018;45(6):368-373.

Cardoso MJ, Leung K, Modat M, et al. STEPS: Similarity and Trush Estimation for Propagated Segmentations and its application to hippocampal segmentation and brain parcellation. Med Image Anal 2003;17:671-684.

Modat M, Ridgway GR, Taylor ZA, Lehmann M, Barnes J, Hawkes DJ, Fox NC, Ourselin S. Fast free-form deformation using graphics processing units. Comput Methods Programs Biomed 2010;98:278–84

Modat M, Cash DM, Daga, P, Winston GP, Duncan JS, Ourselin S. Global image registration using a symmetric block-matching approach. J Med Imaging 2014;1(2):024003
Scott RC, Cross JH, Gadian DG, et al. Abnormalities in hippocampi remote from the seizure focus: a T2 relaxometry study. Brain 2003;126:1968-74.
Briellmann RS, Kalmins RM, Berkovic SF, et al. Hippocampal pathology in refractory temporal lobe epilepsy: T2-weighted signal change reflects dentate gliosis. Neurology 2002;58:265-71.
Von Oertzen J, Urbach H, Blumcke I, et al. Time-efficient T2 relaxometry of the entire hippocampus is feasible in temporal lobe epilepsy. Neurology 2002;58:257-64.
Stefanits H, Springer E, Pataraia E, et al. Seven-tesla MRI of Hippocampal Sclerosis: An in vivo feasibility study with histological correlations. Invest Radiol 2017;52:666-671.
Iglesias JE, Augustinack JC, Nguyen K, et al. A computation atlas of the hippocampal formation using ex vivo, ultra-high resolution MRI : application to adaptive segmentation of in vivo MRI. NeuroImage 2015;115:117-137.
Yushkevich PA, Pluta JB, Wang H, et al. Automated volumetry and regional thickness analysis of hippocampal subfields and medial temporal cortical structures in mild cognitive impairment. Human Brain Mapping 2015;36:258-287.
Sone D, Sato N, Maikusa N, et al. Automated subfield volumetric analysis of hippocampus in temporal lobe epilepsy using high-resolution T2-weighted MR imaging. NeuroImage Clinical, 2016;12:57-64.
Voets NL, Hodgetts CJ, Sen A, Adcock JE, Emir U. Hippocampal MRS and subfield volumetry at 7T detects dysfunction not specific to seizure focus. Scientific Reports 2017;16138.
Kreilkamp BAK, Weber B, Elkommos SB, Richardson MP, Keller SS. Hippocampal subfield segmentation in temporal lobe epilepsy : relation to outcomes. Acta Neurologica Scandinavia 2018;137:598-608
Shah P, Bassett DS, Wisse LEM, et al. Structural and functional asymmetry of medial temporal lobe subregions in unilateral temporal lobe epilepsy: A 7T MRI study. Human Brain Mapping 2019;40:2390-98
Bernhardt BC, Fadaie F, Vos de Wael R, et al. Preferential susceptibility of limbic cortices to microstructural damage in temporal lobe epilepsy: A quantitative T1 mapping study. NeuroImage 2018;182:294-303.
Galovic M, Baudracco I, Wright-Goff E, et al. Association of Piriform Cortex Resection with Surgical Outcome in Patients with Temporal Lobe Epilepsy. JAMA Neurol 2019 in press
Sidhu M, Stretton J, Winston GP, et al. Memory network reorganization after temporal lobe resection: a longitudinal functional imaging study. Brain 2016;139:415-430
Bernasconi A, Cendes F, Theodore WH, et al. Recommendations for the use of structural magnetic resonance imaging in the care of patients with epilepsy: A consensus report from the International League Again Epilepsy Neuroimaging Task Force. Epilepsia 2019 in press.
Goubran M, Bernhardt BC, Cantor-Rivera D, et al. In vivo MRI signatures of hippocampal subfield pathology in intractable epilepsy. Human Brain Mapping 2015;37:1103-1119.
Yoo JG, Jakabek D, Ljung H, et al. MRI morphometry of the hippocampus in drug-resistant temporal lobe epilepsy: Shape inflation of left hippocampus and correlation of right-sided hippocampal volume and shape with visuospatial function in patients with right-sided TLE. J Clin Neurosci 2019 in press.
Hakimi M, Ardekani BA, Pressl C, et al. Hippocampal volumetric integrity in mesial temporal lobe epilepsy: a fast novel method for analysis of structural MRI. Epilepsy Res 2019;154:157-62

Costa BS, Santos MCV, Rosa DV, Schutze M, Miranda DM, Romano-Silva MA. Automated evaluation of hippocampal subfields volume in mesial temporal lobe epilepsy and its relationship to the surgical outcome. Epilepsy Research 2019;154:152-156.

Figure legends

Figure 1: a) The MNI-152 template is reoriented so that the hippocampi are along the A-P axis (realigned MRI, rMRI). b) All healthy controls were registered to this in a groupwise way to generate a group template image. c) A brain mask (yellow) excluding the hippocampi is generated for the group template to drive the non-linear registration between template and subject (d). The distance map (c) from the template is resampled to the subject space (d) and evaluated at each slice within the hippocampal segmentations, red volumes in (d).

Figure 2: A raw 3D-T1 image of a healthy control with hippocampal segmentations is shown in the top row, in a sagittal (left panel) and axial (right panel) view. After rigid rotation to the group template (second row) the hippocampal long axis is along the posterior-anterior (P-A) axis. The cross-sectional area (CSA) and T2 profiles are shown in the third row in a black line and black crosses, respectively, over the normative range (blue shaded area). The two red arrows indicate cuts through the hippocampus at the body (solid arrowhead) and the head (open arrowhead), as shown in the bottom row (T1 left, T2-map right).

Figure 3: Average cross-sectional area (CSA, top row) and T2 (bottom row) profiles per subject group. The blue dashed line is the average of the healthy controls, and the blue shaded area around that the normative range from these controls. The average profiles for each of the three patient groups (LHS in red, RHS in black, and BHS in green) show decreased CSA along much of the length of the hippocamps. The asterisks indicate that at that point the patient profile was below the normative range of the controls ($\mu \pm 1.96\sigma$).

Figure 4: Comparisons of intersubject variability (population-based standard deviation) in CSA (top row) and T2 (bottom row) compared to intrasubject variability (scan-rescan) along the length of the hippocampus in twenty controls.

Figure 5: Example profiles of radiologically-defined unilateral HS without volume or qT2 abnormalities on the whole-hippocampal level.
a) Patient with left HS, had a hippocampal volume just within the normative range (2.40 / 2.84 ml ipsi/contralateral, control range 2.40-3.39 ml) and normal qT2 (112.8 / 116.4 ms ipsi/contralateral, control range 108.5-123.8 ms). CSA and T2 profiles show a clear volume asymmetry primarily anteriorly.
b) Patient 2 with right HS who had normal volumes (2.41 / 3.29 ml ipsi/contralateral, control range 2.40-3.39 ml) and qT2 (118.9 / 112.2 ms ipsi/contralateral, control range 108.5-123.8 ms). CSA and T2 profiles show a clear anterior abnormality in both the CSA and T2 plots.

Figure 6: Examples cases without radiological diagnosis of HS but with HS on histopathology.
a) Patient 2 from Table S1, with left TLE and normal hippocampal volumes (2.52 / 2.93 ml for ipsi/contralateral, control range 2.40-3.39 ml) and qT2 (116.3 / 117.1 ms for ipsi/contralateral, control range 108.5-123.8 ms). The CSA profiles show asymmetry along a big proportion of the length of the hippocampus, with significantly smaller CSA along part of the head and body of the hippocampus. No qT2 abnormalities observed anywhere along the profile. b) Patient 4 from Table S1 with left TLE and normal hippocampal volumes (2.69 / 3.01 ml for ipsi/contralateral, control range 2.40-3.39 ml) and qT2 (123.5 / 115.1 ms for ipsi/contralateral, control range 108.5-123.8 ms). CSA profiles show slightly larger than

normal volumes along the head and body of the hippocampus, with asymmetry along the body with predominantly lower cross-sectional area in the ipsilateral, left, hippocampus. This corresponds with significantly elevated ipsilateral qT2 values on three consecutive slices.

a)

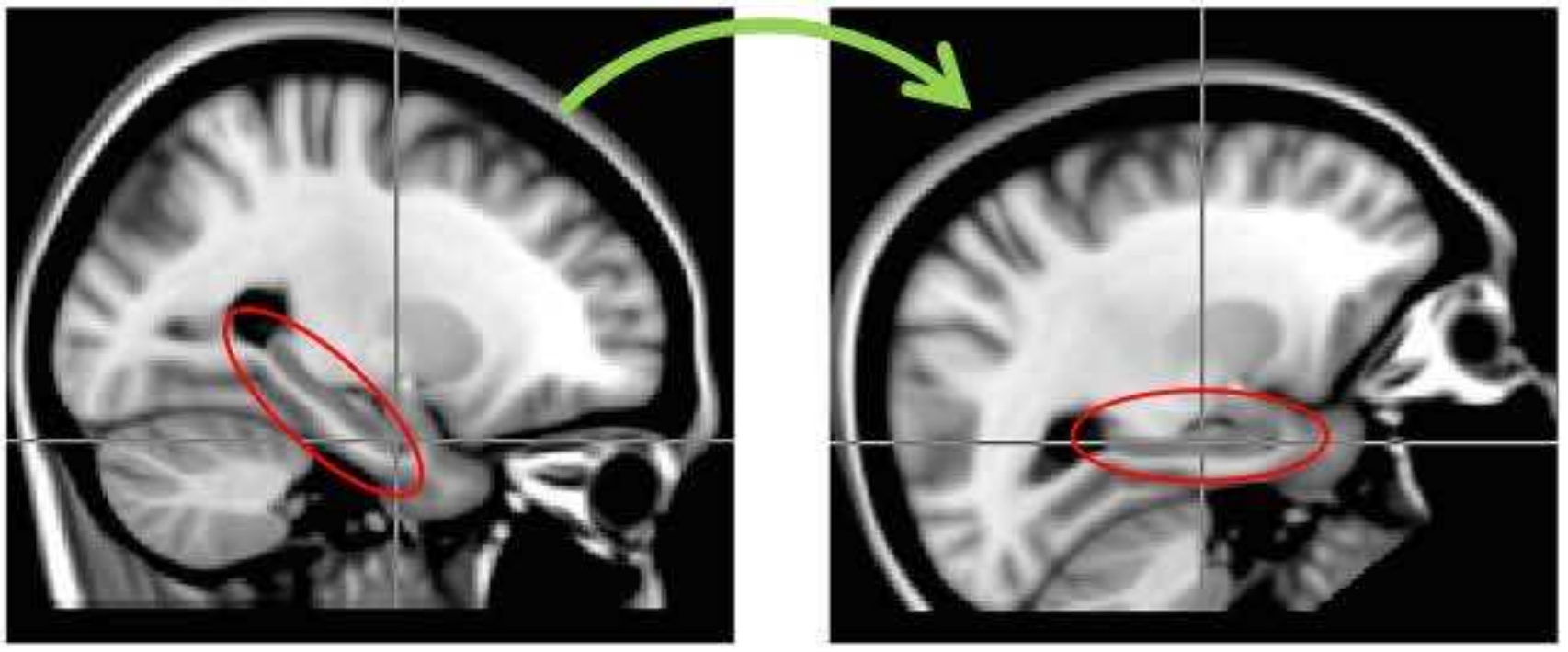

MNI Realigned MNI (rMNI)

b)

Group template

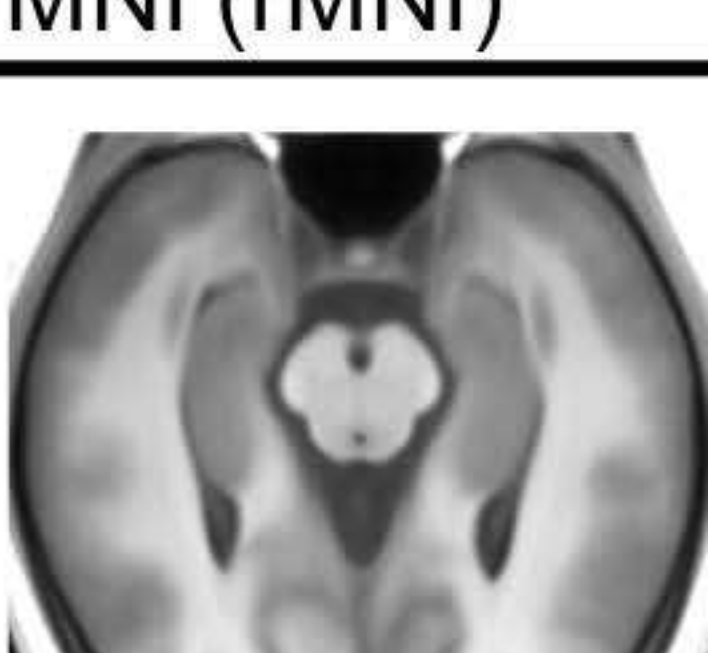

c)

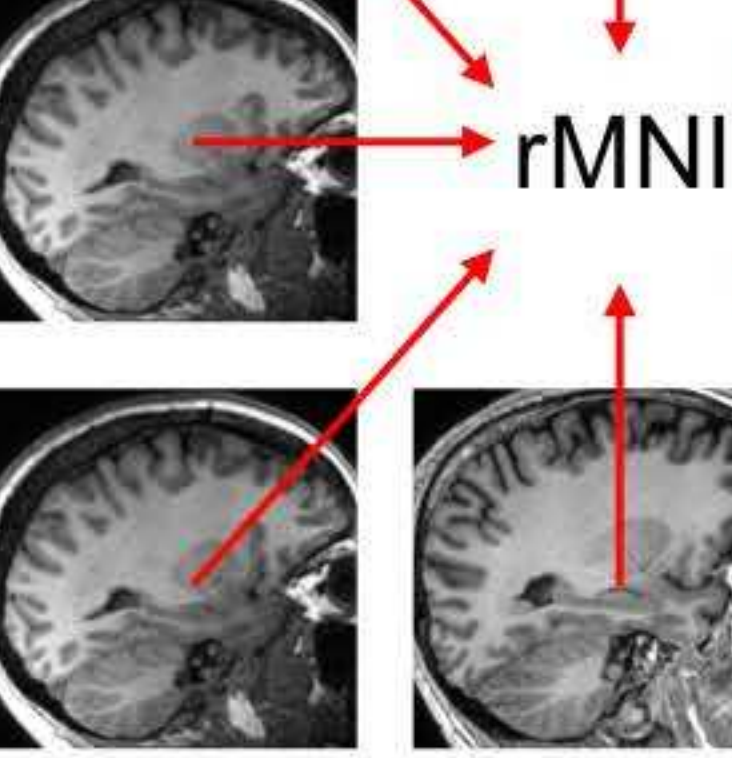

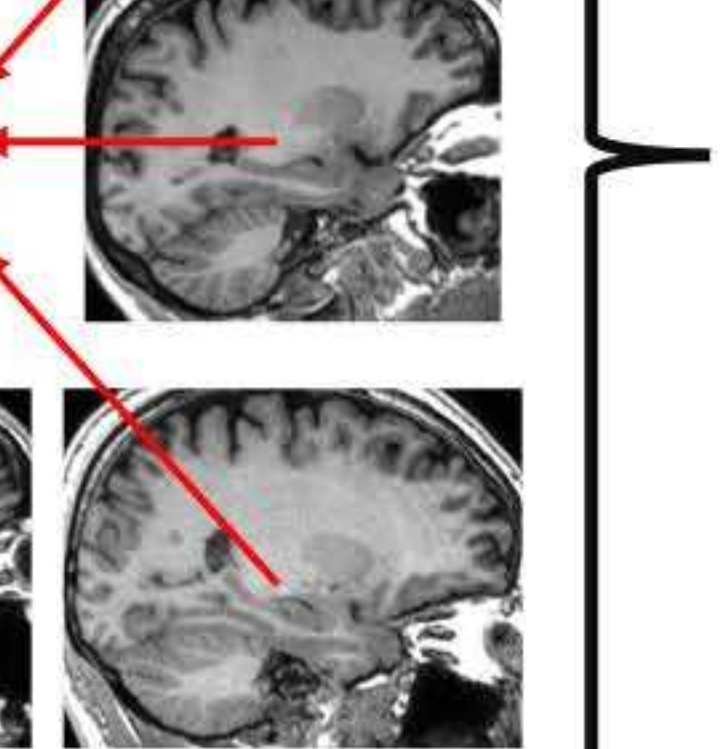

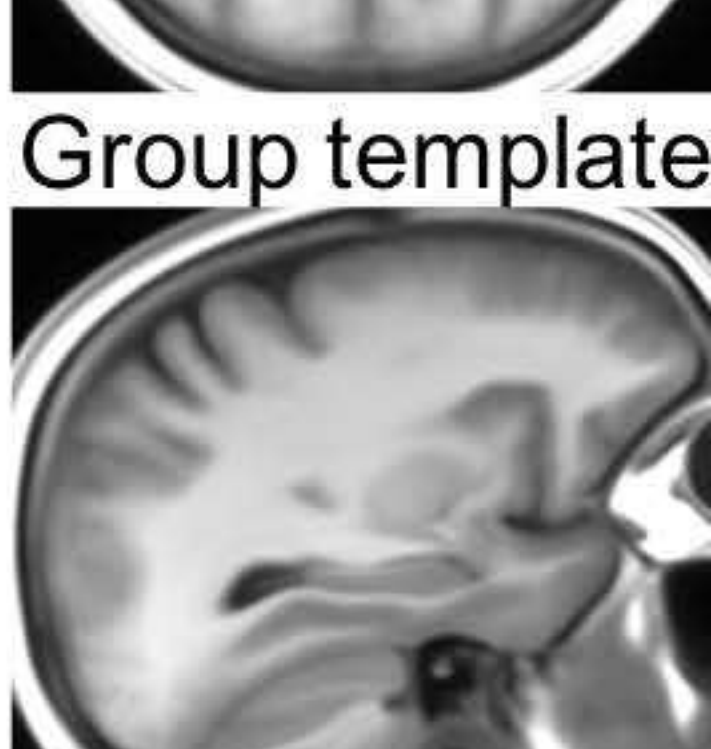

d)

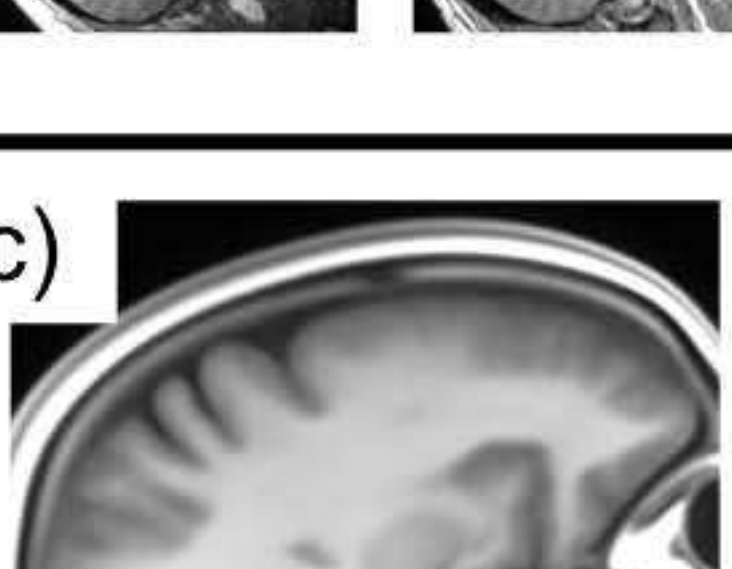

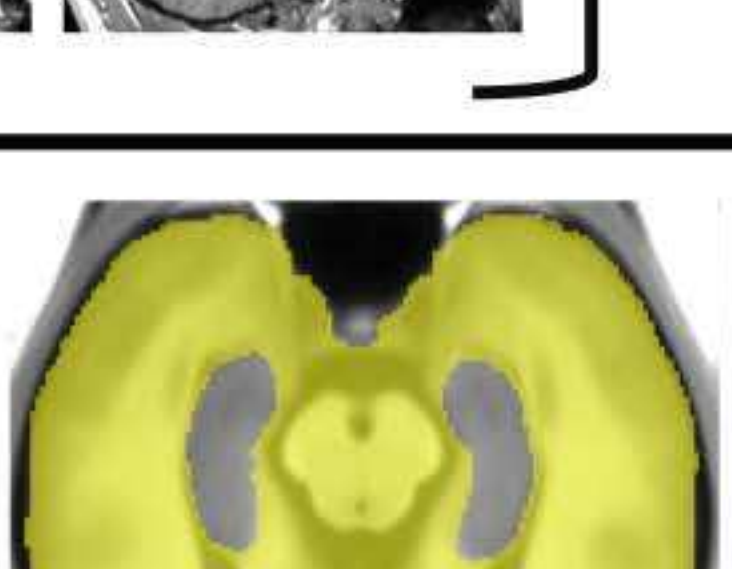

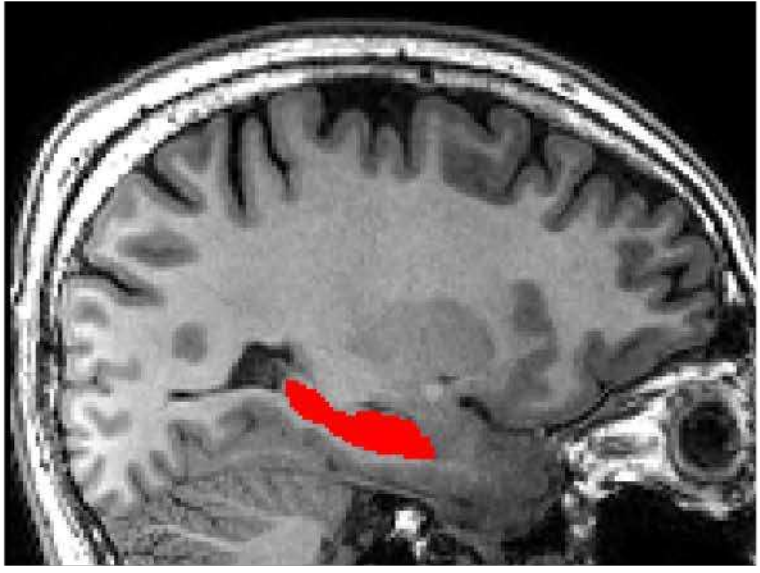

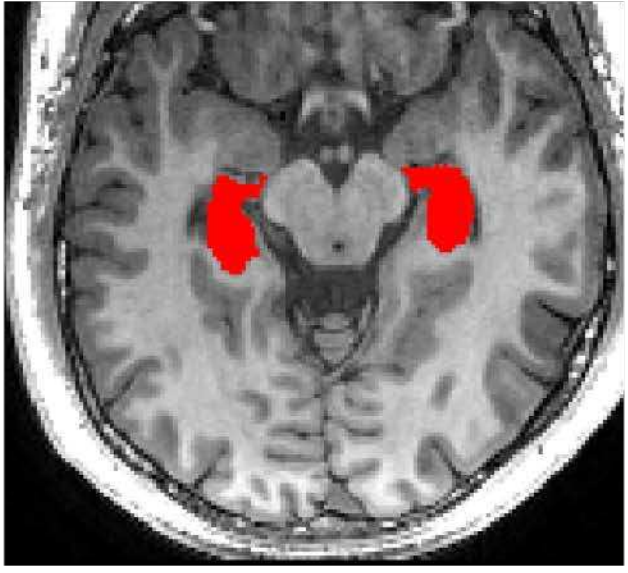

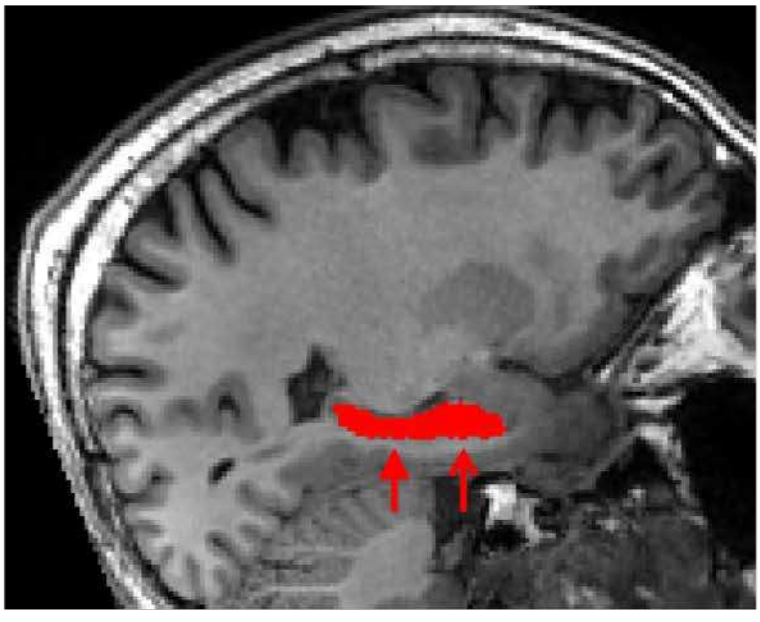

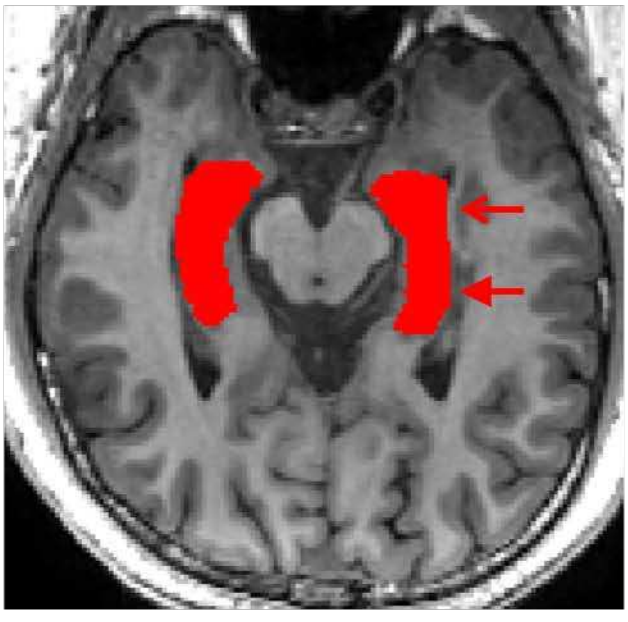

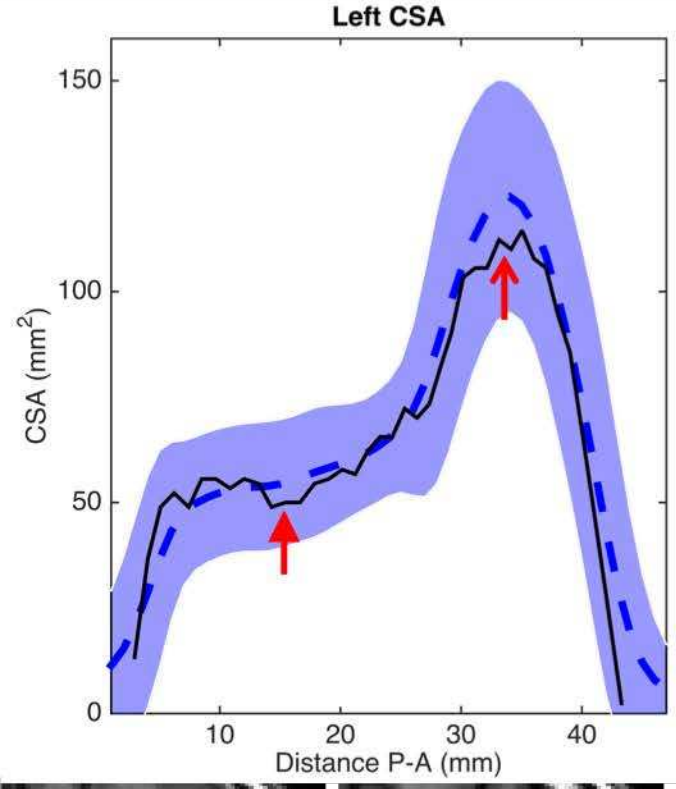
Left CSA
150
100
50
0
CSA (mm^2)
10
20
30
40
Distance P-A (mm)

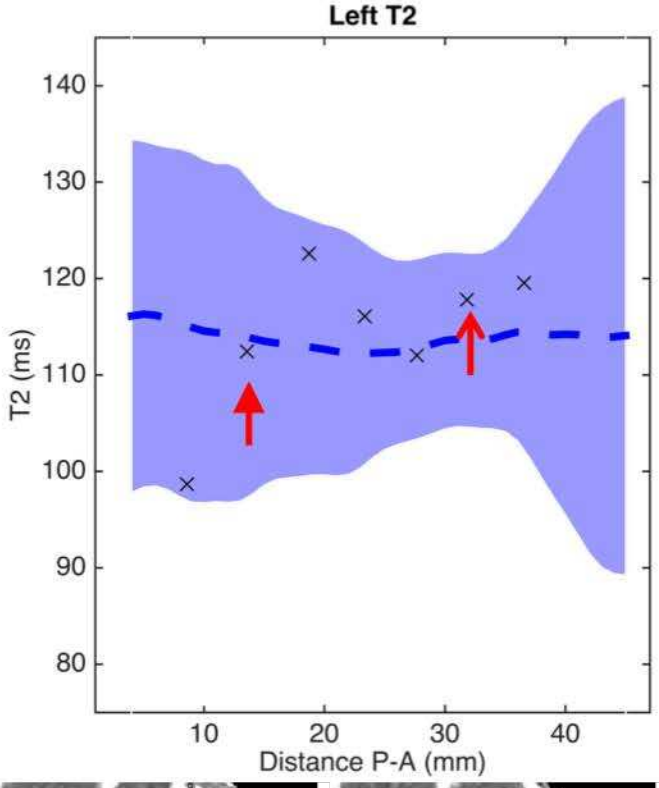
Left T2
140
130
120
110
100
90
80
T2 (ms)
10
20
30
40
Distance P-A (mm)

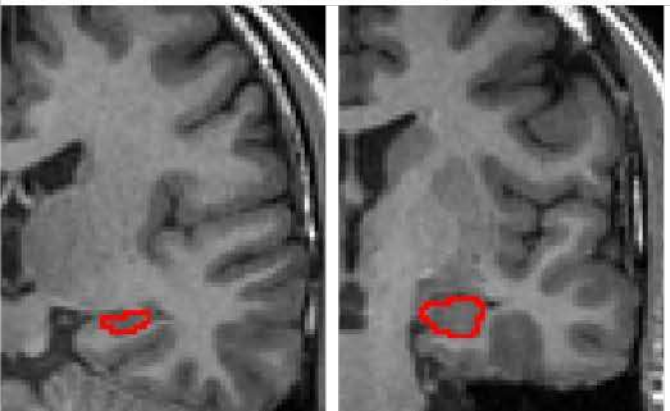

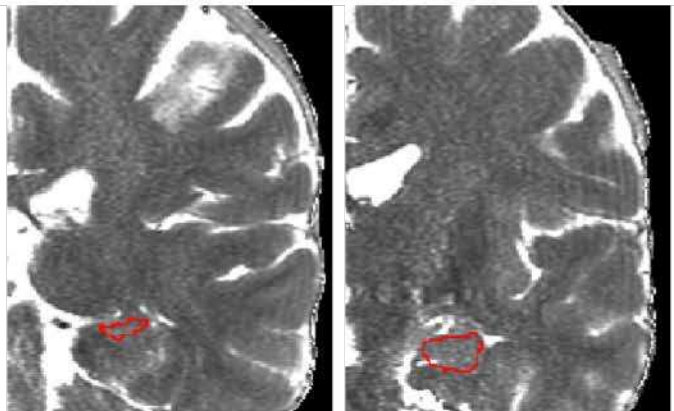

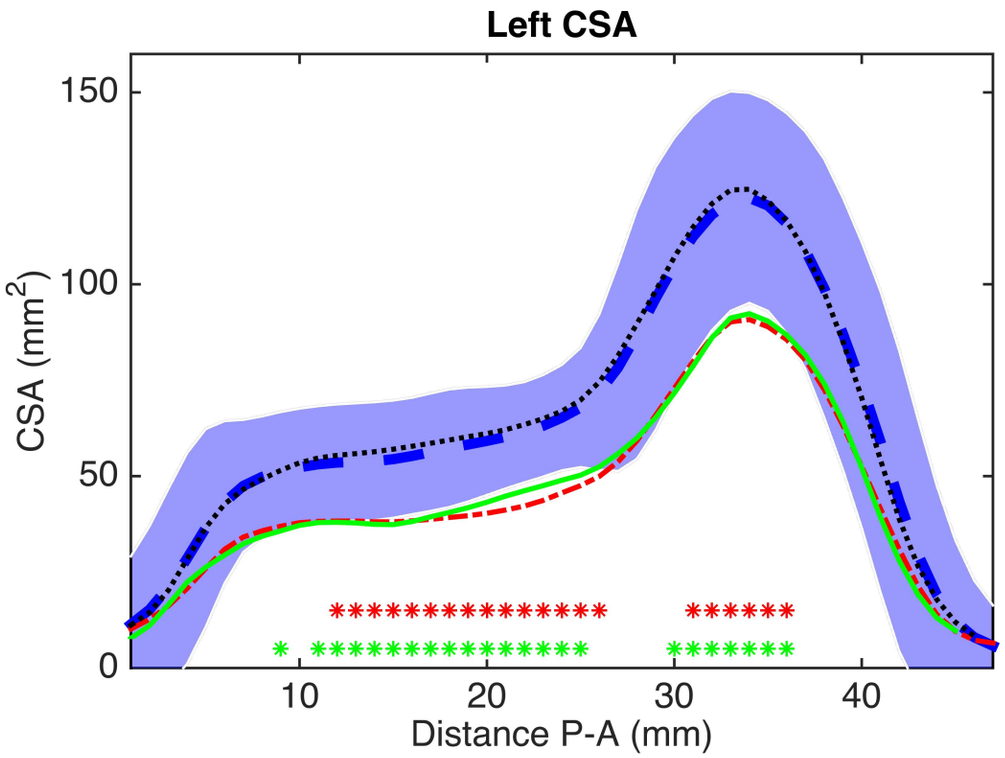
Left CSA
150
100
50
0
CSA (mm2)
10
20
30
40
Distance P-A (mm)

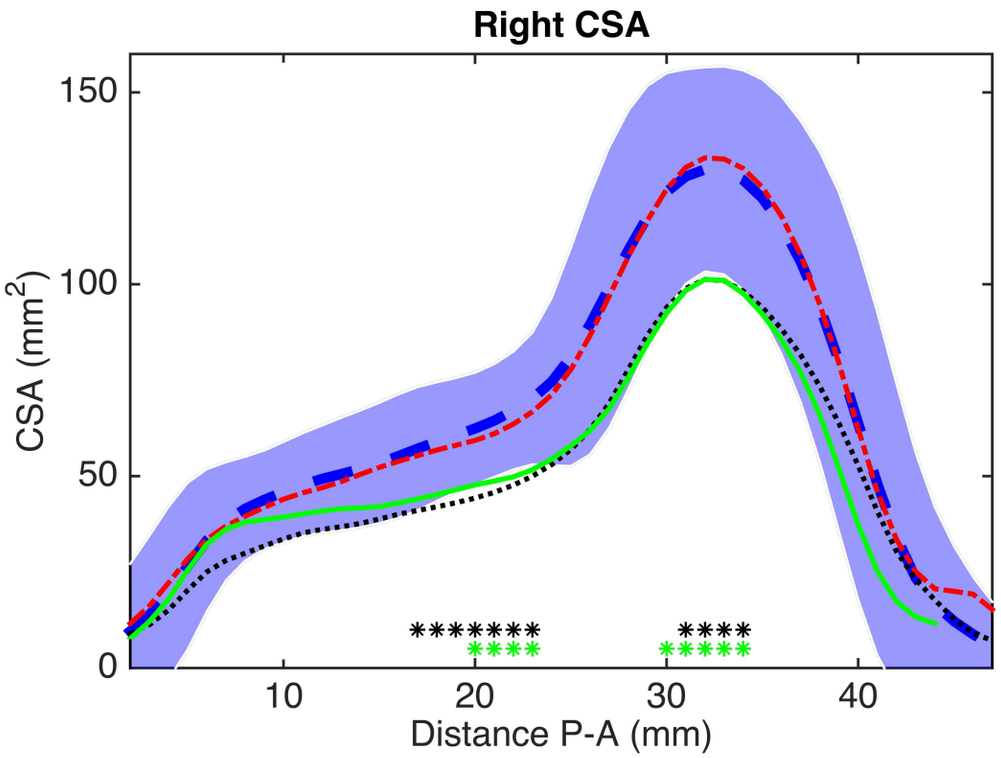
Right CSA
150
100
50
0
CSA (mm2)
10
20
30
40
Distance P-A (mm)

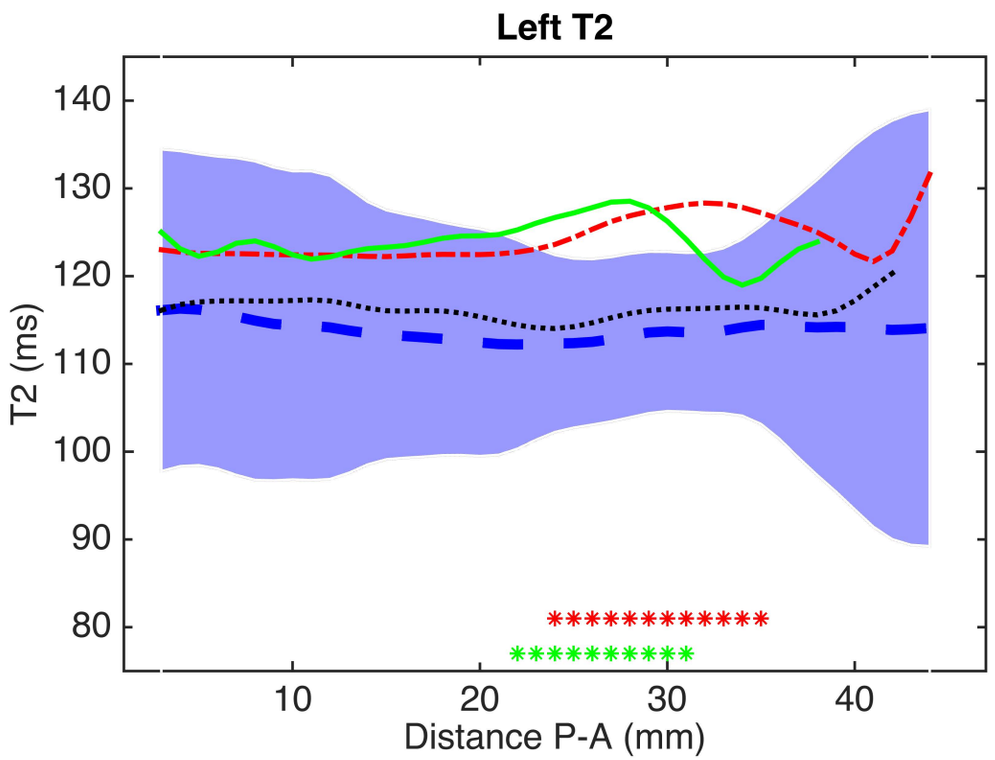
Left T2
140
130
120
110
100
90
80
T2 (ms)
10
20
30
40
Distance P-A (mm)

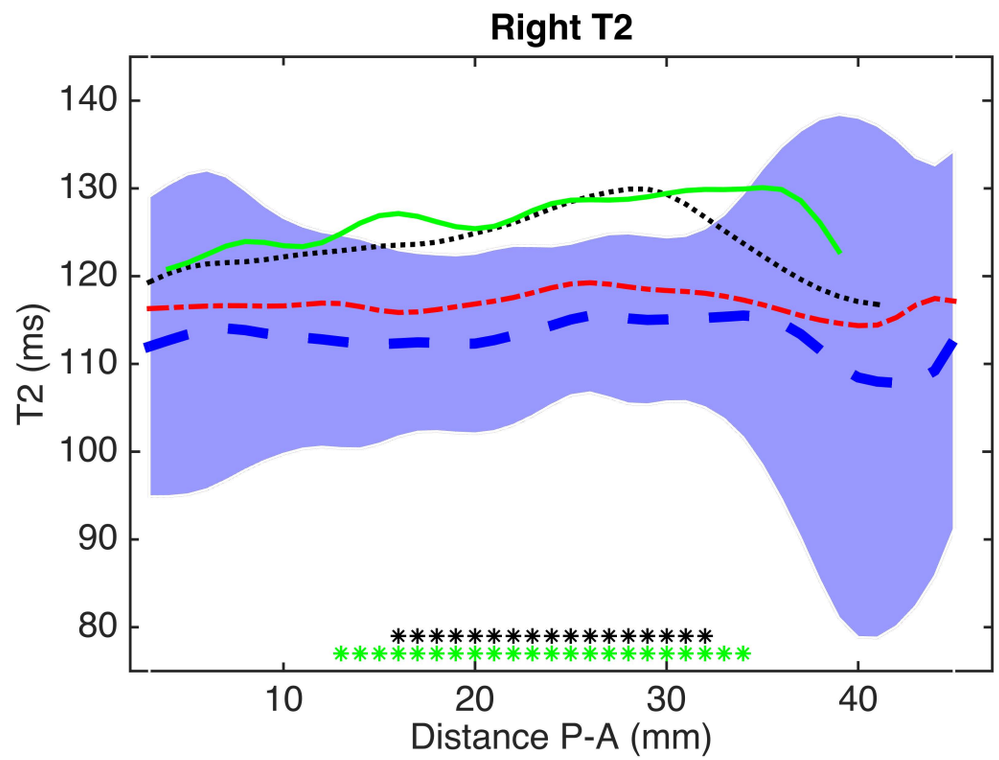
Right T2
140
130
120
110
100
90
80
T2 (ms)
10
20
30
40
Distance P-A (mm)

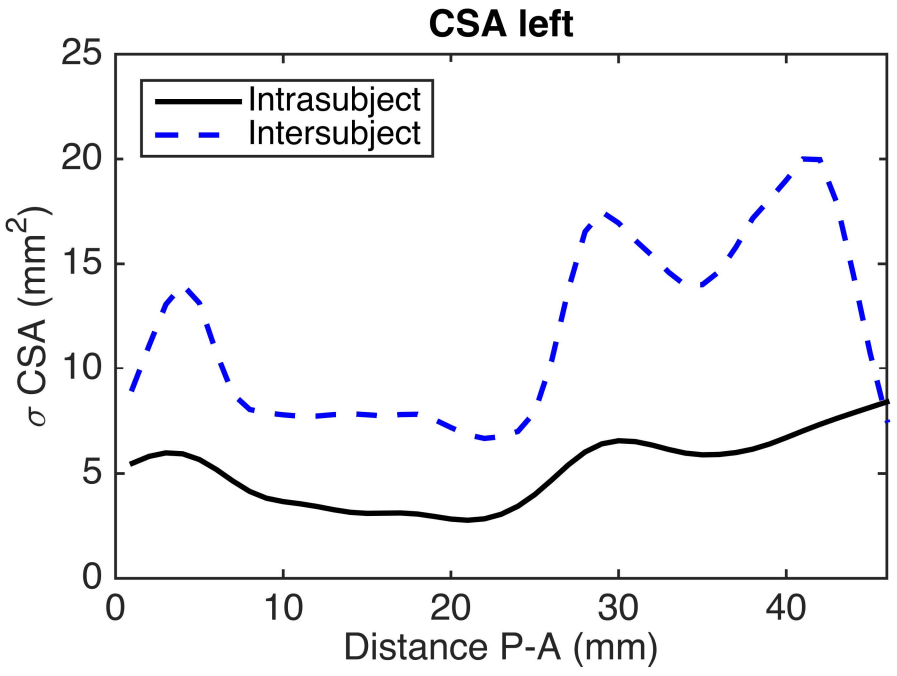
CSA left
Intrasubject
Intersubject
σ CSA (mm²)
Distance P-A (mm)
0
5
10
15
20
25
0
10
20
30
40

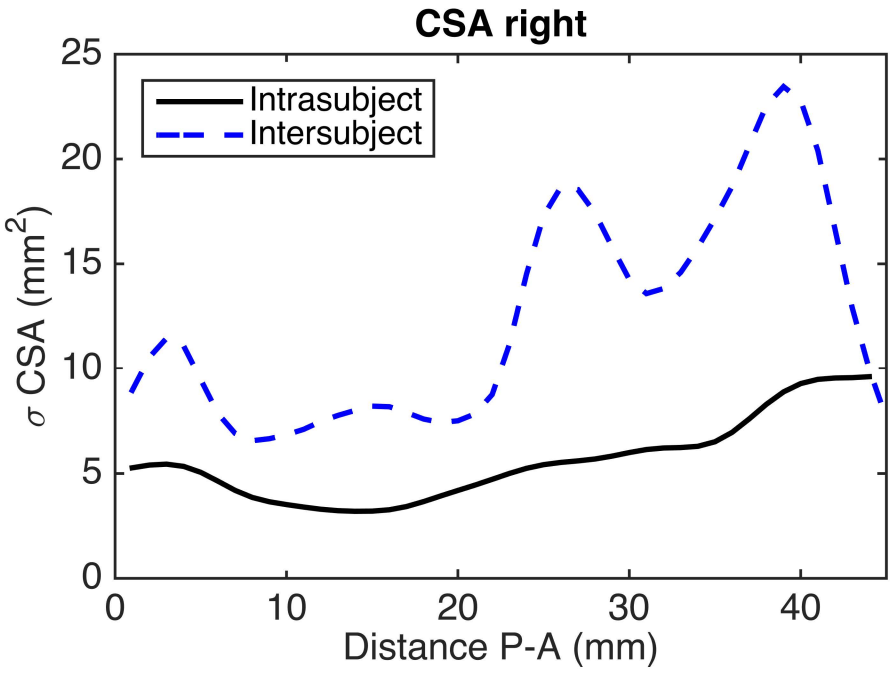
CSA right
Intrasubject
Intersubject
σ CSA (mm²)
Distance P-A (mm)
0
5
10
15
20
25
0
10
20
30
40

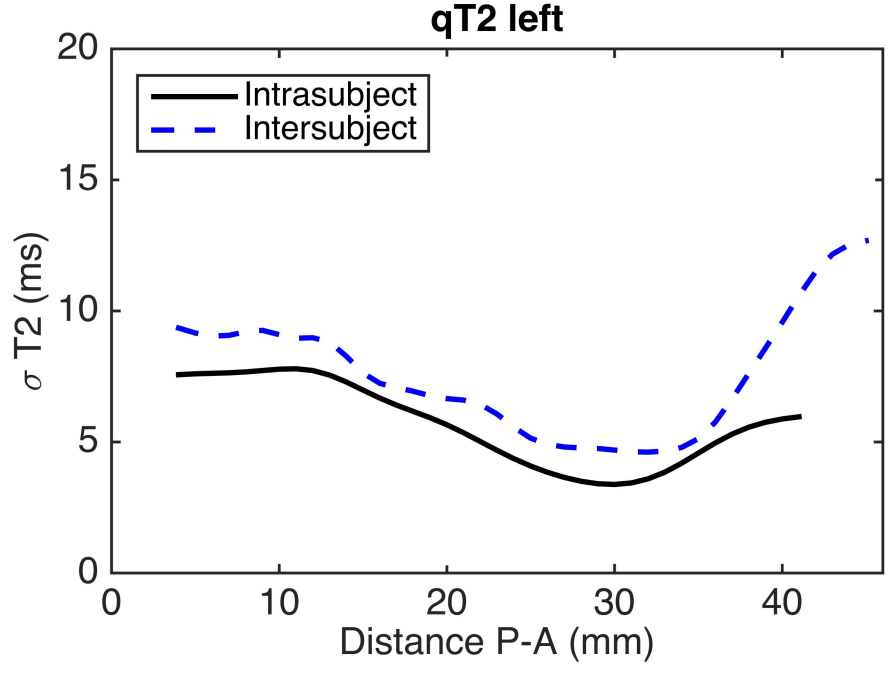
qT2 left
Intrasubject
Intersubject
σ T2 (ms)
Distance P-A (mm)
0
5
10
15
20
0
10
20
30
40

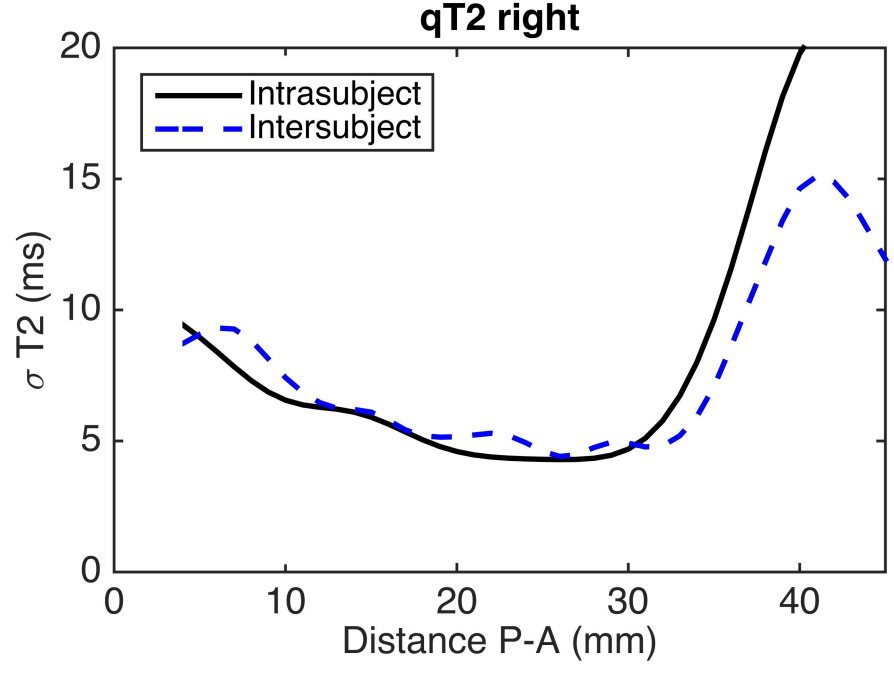
qT2 right
Intrasubject
Intersubject
σ T2 (ms)
Distance P-A (mm)
0
5
10
15
20
0
10
20
30
40

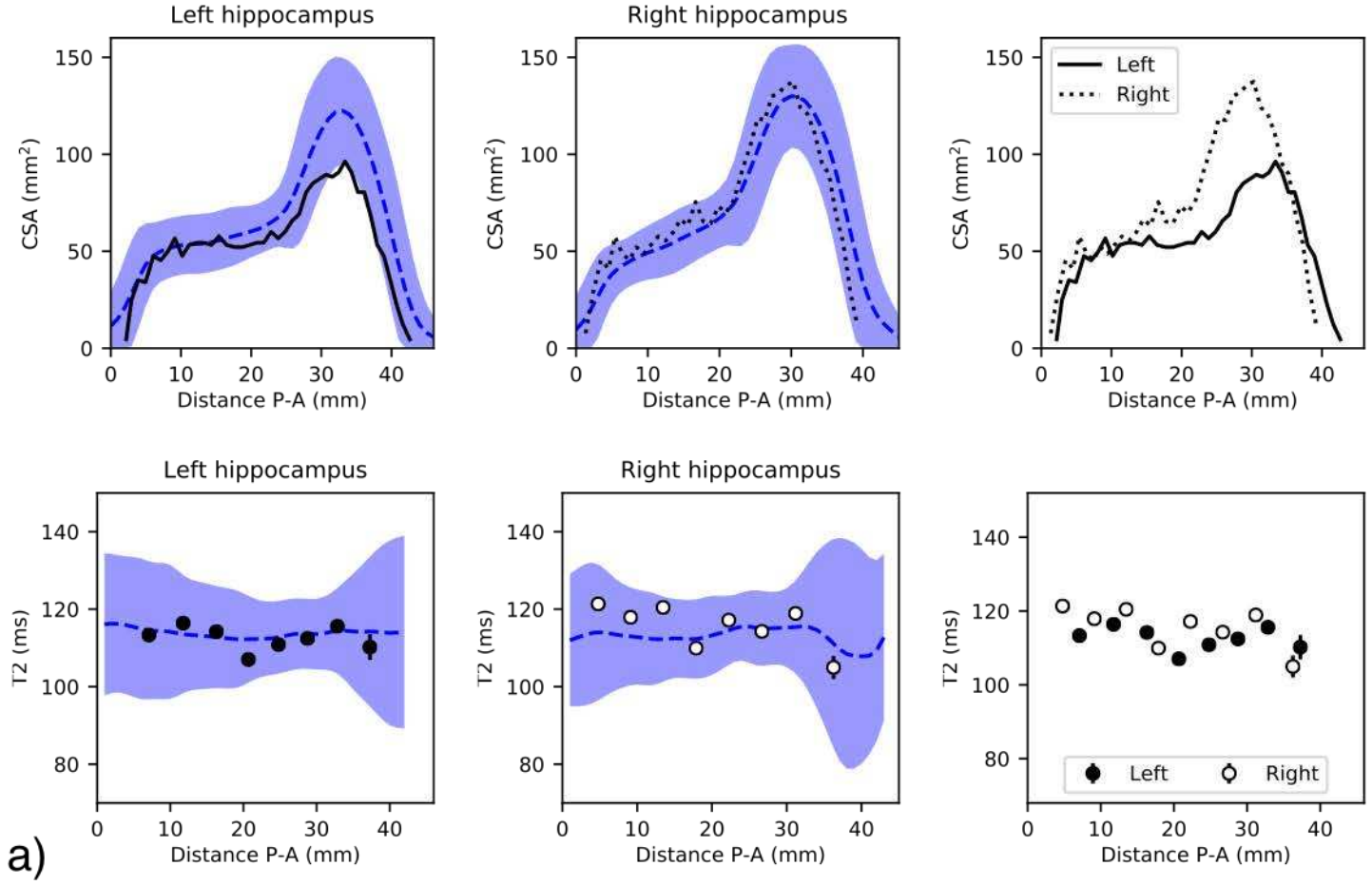
Left hippocampus
Right hippocampus
CSA (mm²)
Distance P-A (mm)
Left
Right
T2 (ms)
a)

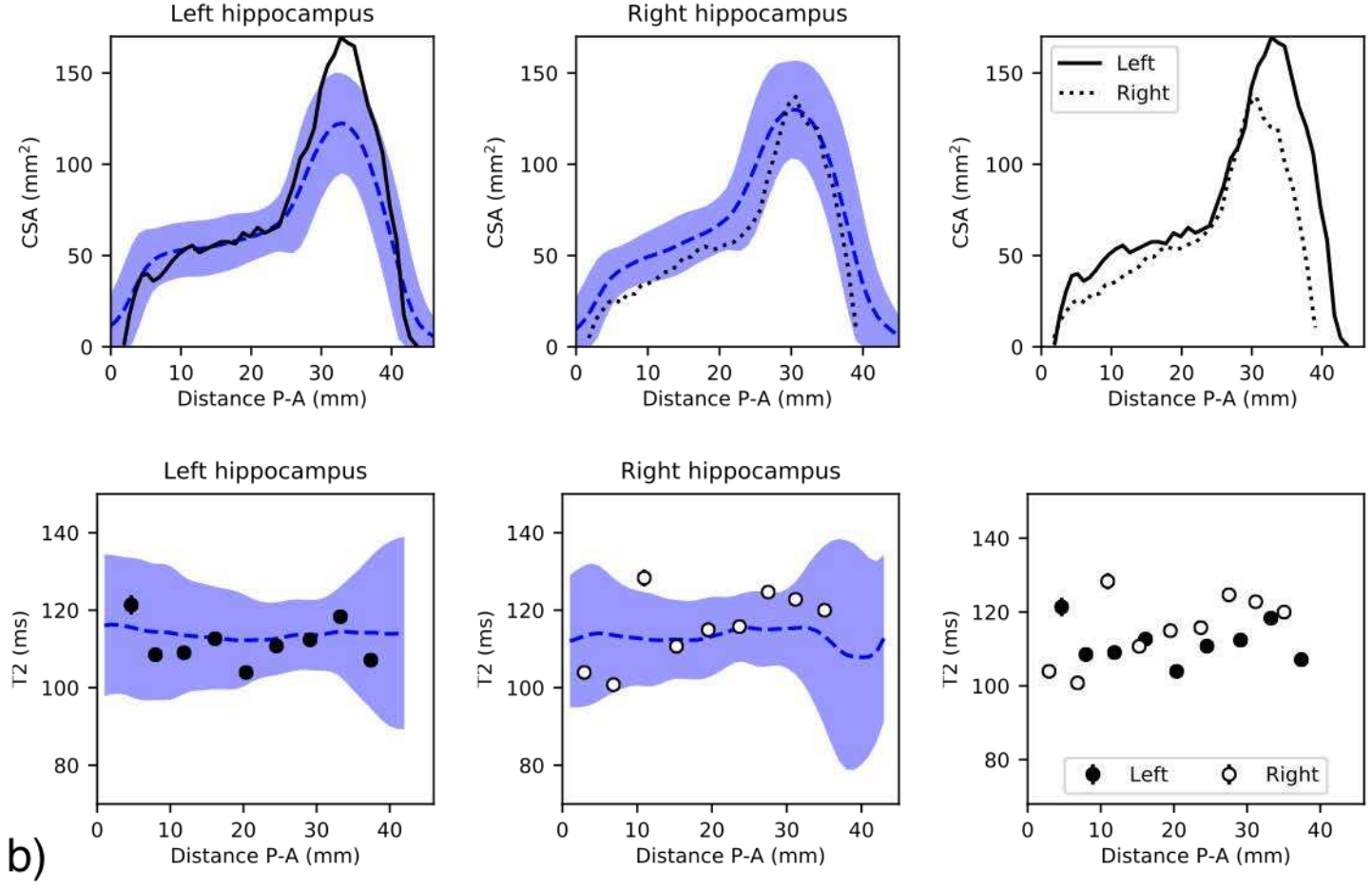
Left hippocampus
Right hippocampus
CSA (mm²)
Distance P-A (mm)
Left
Right
T2 (ms)
b)

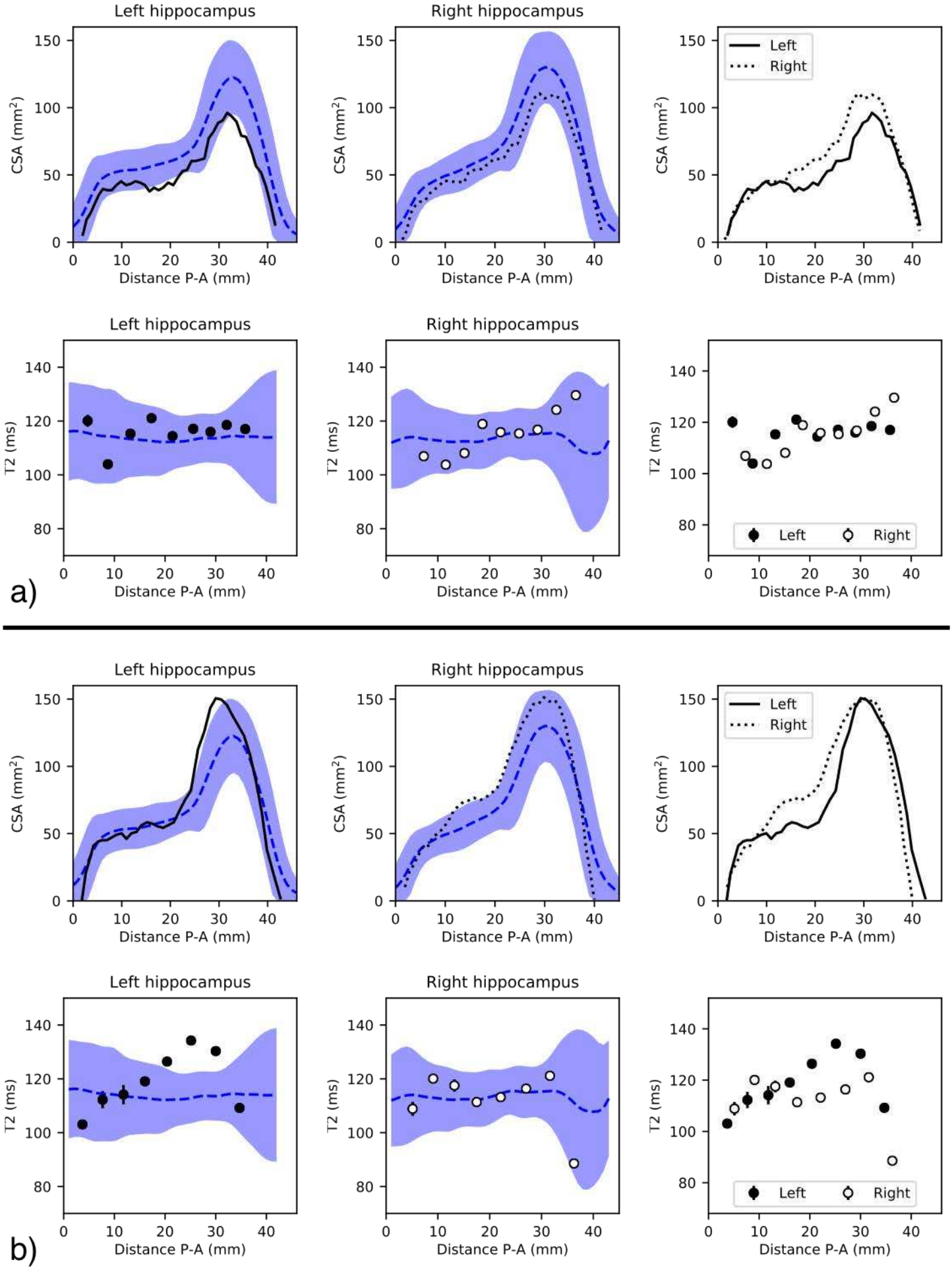
Left hippocampus
Right hippocampus
CSA (mm²)
Distance P-A (mm)
Left
Right
T2 (ms)
a)
b)


a)

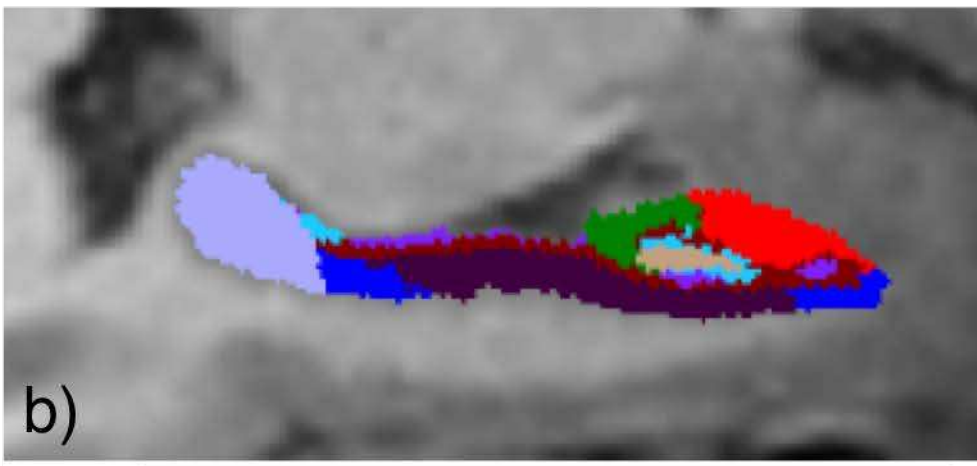
b)

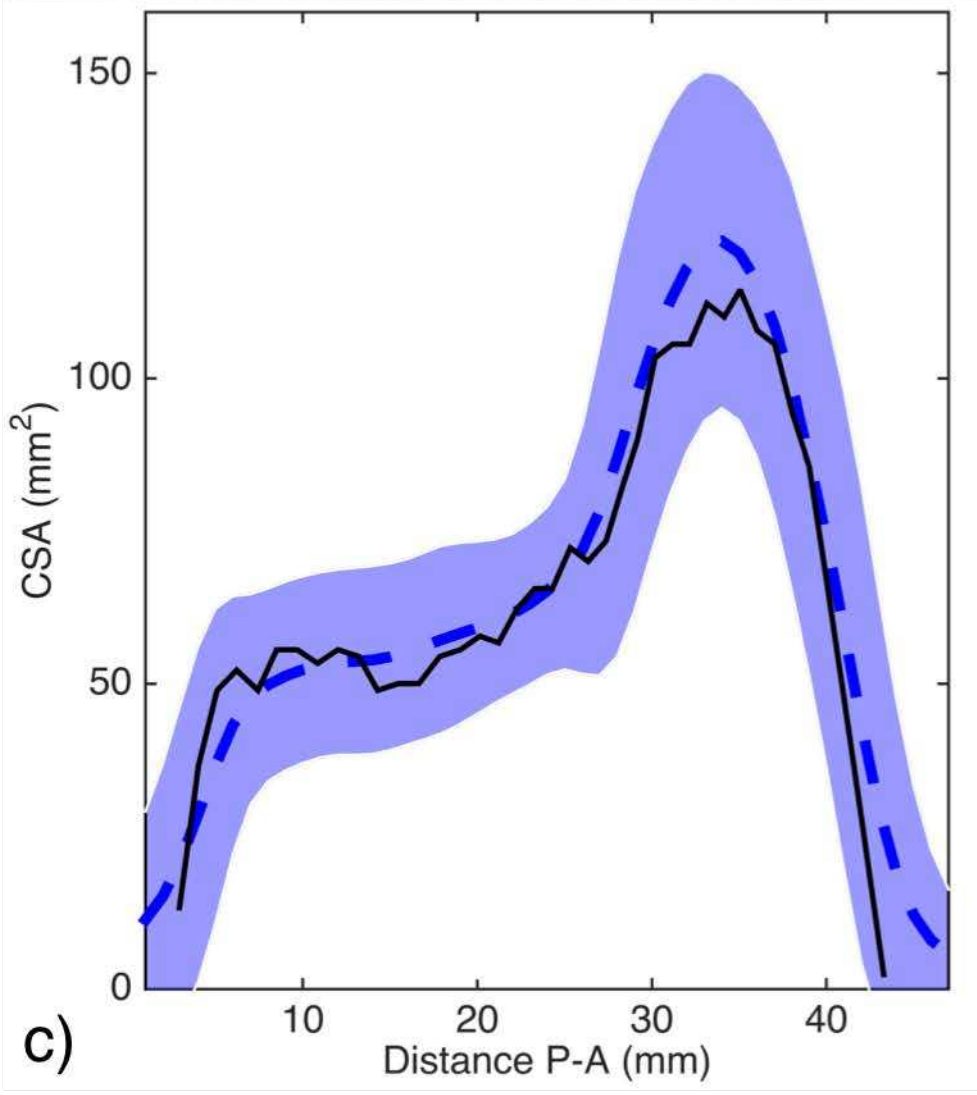
150
100
50
0
CSA (mm^2)
10
20
30
40
Distance P-A (mm)
c)

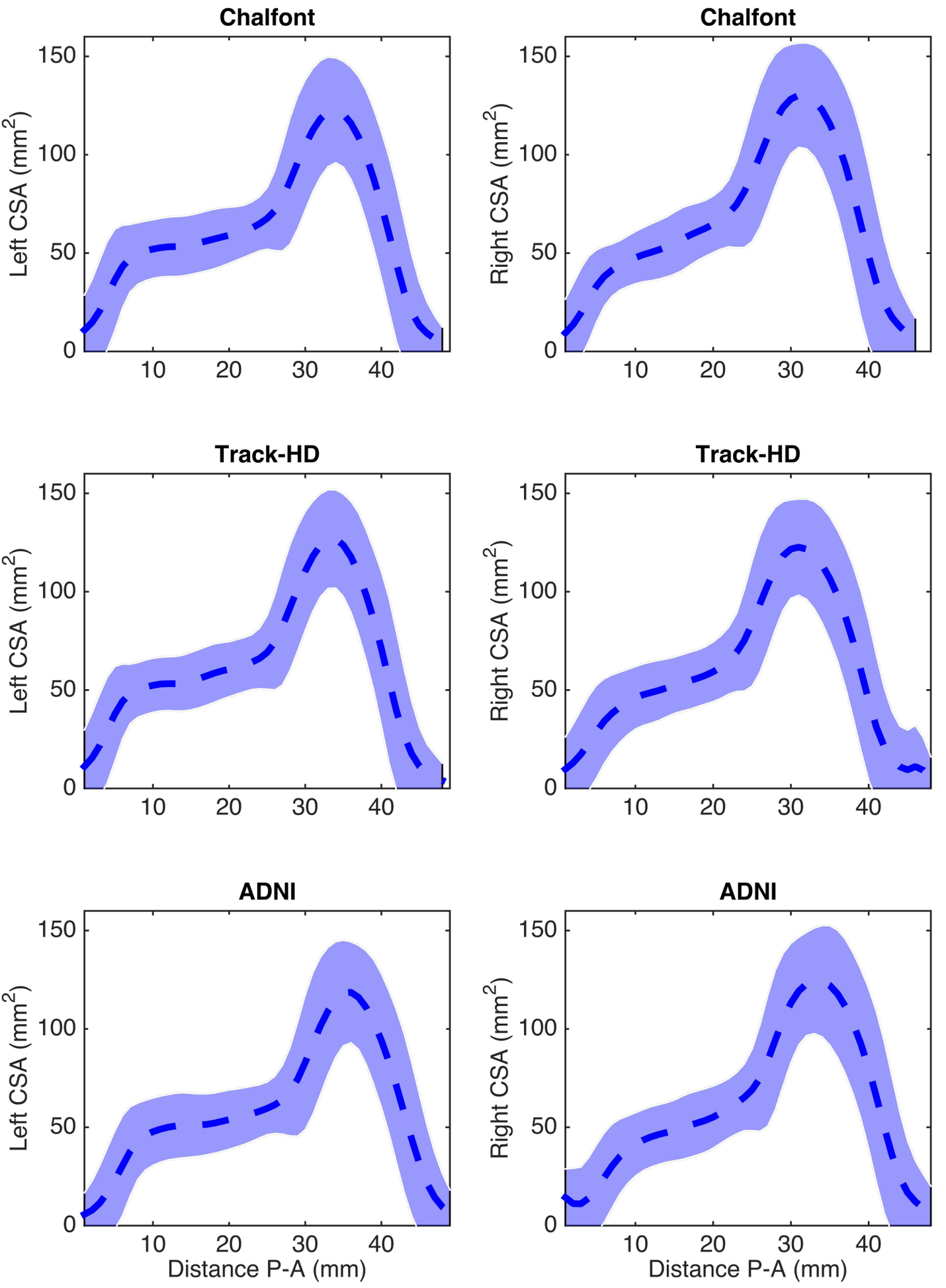
Chalfont
Left CSA (mm2)
Chalfont
Right CSA (mm2)
Track-HD
Left CSA (mm2)
Track-HD
Right CSA (mm2)
ADNI
Left CSA (mm2)
Distance P-A (mm)
ADNI
Right CSA (mm2)
Distance P-A (mm)
0
50
100
150
10
20
30
40

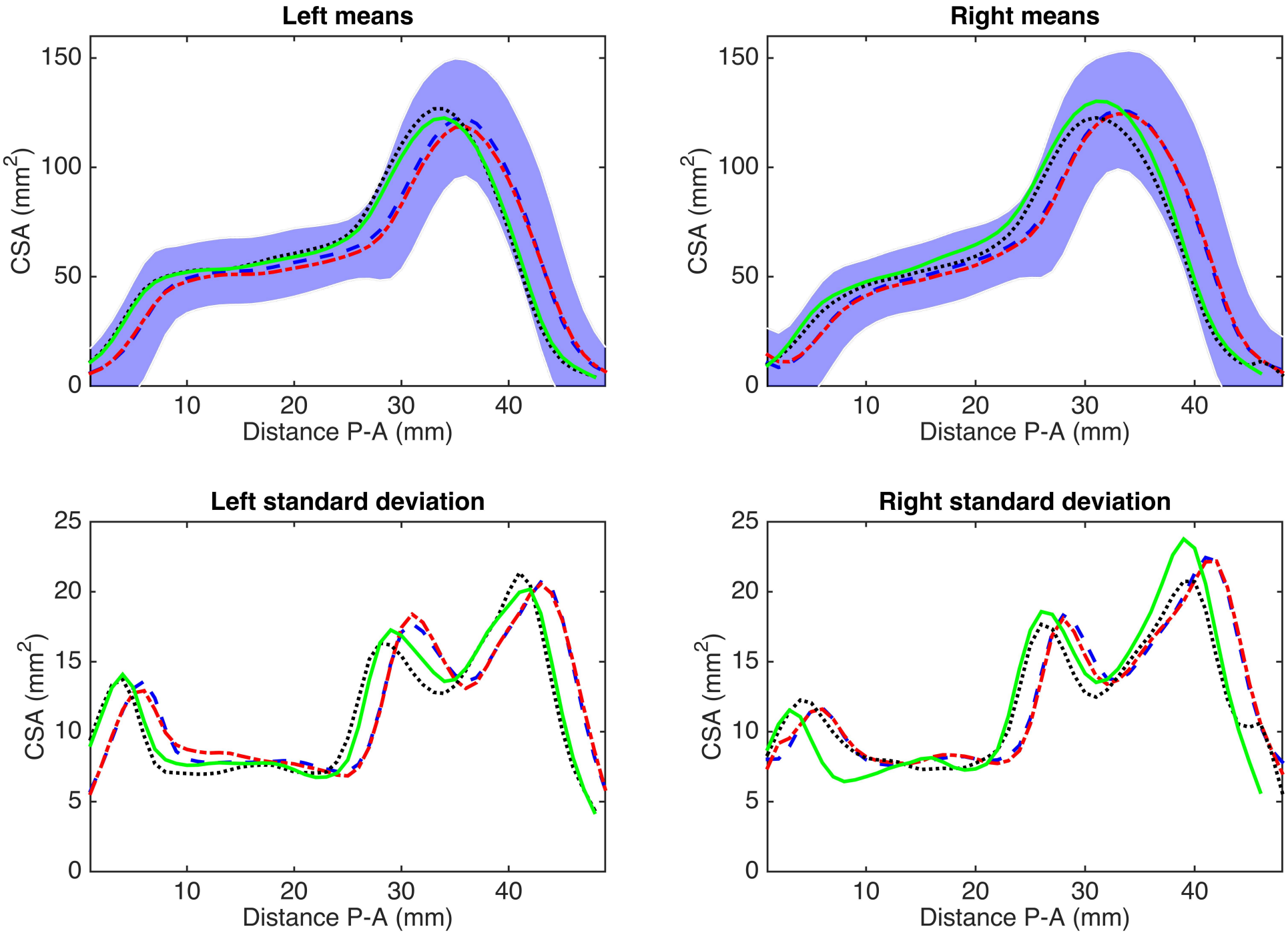
Left means
Right means
Left standard deviation
Right standard deviation
CSA (mm^2)
Distance P-A (mm)
0
50
100
150
5
10
15
20
25
10
20
30
40

Supplementary material

Hippocampal subfield segmentation

The healthy control shown in Fig. 2 was processed with FreeSurfer v6.0.0 using the automated hippocampal segmentation method (Iglesias et al., 2015) and aligned with the template image to visualise the association of the subfields with the hippocampal CSA profiles (Fig. S1).

Generalisation

For generalisability to an online tool, we included two publicly available 3T imaging datasets: Alzheimer's Disease Neuroimaging Initiative (ADNI) and Track-HD (Tabrizi et al., 2012). TRACK-HD T1-weighted image volumes were acquired using a 3D MPRAGE acquisition sequence on 3.0 T Siemens and Phillips scanners with a voxel size of 1.10×1.10×1.10 (Philips) and 1.07×1.07×1.10 (Siemens). This included a total of 98 subjects (age μ±σ 46.6±10.7, range 23.0-65.7 years; 43M/55F). The 3T ADNI data were acquired at multiple scanners and scans were only excluded for image quality reasons. Voxel size for these 3D MPRAGE/IR-FSPGR acquisition varied between 1.00×1.00×1.20 to 1.05×1.05×1.20 mm (see http://adni.loni.usc.edu/methods/documents/mri-protocols/ for imaging details), leading to a total of 217 subjects. To match sample sizes to the Chalfont and Track-HD populations, 109 randomly selected subjects were taken (age μ±σ 73.7±5.7, range 59.9-86.0 years; 50M/59F).

The methodology of processing these additional datasets was identical to the main manuscript. Fig. S2 shows the comparison of the normative ranges for both left and right hippocampi in individual plots. Fig. S3 shows the averages and standard deviations of the three populations in a single plot. Comparing the three datasets, the mean CSA along the hippocampal long axis varies very little despite the generally higher age in the ADNI database (Fig. S3a,b). Similarly, the same regions of increased variability are seen (Fig. S3c,d) and little difference in the magnitude of variation. As a result, we feel justified in combining all three of these populations.

***Supplementary Table S1**: Details of patients without HS as radiological diagnosis*

	Age at scan	Age at surgery	Radiological diagnosis	Pathological report
Patient 1 (F)	27.0 y	27.4 y	R amyg lesion – DNT?	DNT (GG,GR 1), HS (EFS)
Patient 2 (F)	28.1 y	28.8 y	L amyg lesion – DNT?	DNT (GNT), HS type 1
Patient 3 (F)	48.2 y	48.4 y	Subtle increase in T2 signal in R amyg and hippocampal head	HS type 2
Patient 4 (F)	37.6 y	37.7 y	L hippocampal bowel asymmetry, no convincing signal alteration	HS type 1
Patient 5 (M)	60.8 y	62.3 y	Cavernoma abutting left temporal horn	Cavernoma, mild HS type 3

HS = hippocampal sclerosis ; F = female, m = male; R = right; L = left; Amyg = amygdala; DNT = Dysembryoplastic neuroepithelial tumour;

***Supplementary Table S2**: Volume and qT2 of whole hippocampi*

	HC (n=111)	LHS (n=32)	RHS (n=32)	BHS (n=5)
Left volume (ml)	2.87 ± 0.26	1.92 ± 0.35*	2.83 ± 0.21	1.95 ± 0.23*
Right volume (ml)	2.92 ± 0.25	2.82 ± 0.29	2.07 ± 0.28*	2.14 ± 0.31*
Left qT2 (ms)	112.7 ± 11.4	125.1 ± 6.9*	115.9 ± 4.7^	124.6 ± 7.3*
Right qT2 (ms)	113.4 ± 11.5	117.8 ± 3.1*	126.0 ± 6.2*	127.7 ± 3.5*

HC = healthy controls; LHS = left HS; RHS = right HS; BHS = bilateral HS; qT2 = quantitative T2; * indicates $p<0.001$ with respect to HC; ^ $p=0.0026$ with respect to HC.

Supplementary figure legends

Figure S1: A sagittal slice through the left hippocampus (a), with the subfields colour-coded (b), and the associated cross-sectional area (CSA) profile (c). The subfield colours are: CA1=red, CA2=, CA3=green, CA4=brown, molecular layer=maroon, dentate gyrus=aqua, presubiculum=dark purple, subiculum=dark blue, tail=light purple.

Figure S2: Mean and normative ranges shown for cross-sectional area (CSA) plot from three different healthy control cohorts: a local Chalfont one, from the Track-HD study, and from ADNI.

Figure S3: The normative range (blue shaded area) of the entire healthy control population from the three different cohorts, with the mean shown as a dashed blue line, for the CSA of the left (a) and right (b) hippocampus. The mean CSA profiles for the three cohorts are shown: local cohort (solid green line), ADNI (red dashed-dotted line), and Track-HD (black dotted line). Panels c and d show the standard deviations along the PA-axis, with the same colour-encoding per line.